1521-0111/86/3/306–317$25.00
MOLECULAR PHARMACOLOGY

http://dx.doi.org/10.1124/mol.114.093377
Mol Pharmacol 86:306–317, September 2014

The Novel $\alpha_7\beta_2$-Nicotinic Acetylcholine Receptor Subtype Is Expressed in Mouse and Human Basal Forebrain: Biochemical and Pharmacological Characterization [S]

Milena Moretti, Michele Zoli, Andrew A. George, Ronald J. Lukas, Francesco Pistillo, Uwe Maskos, Paul Whiteaker, and Cecilia Gotti

CNR Institute of Neuroscience, Biometra University of Milan, Milan, Italy (M.M., F.P., C.G.); Section of Physiology and Neurosciences, Department of Biomedical, Metabolic, and Neural Sciences, University of Modena and Reggio Emilia, Modena, Italy (M.Z.); Division of Neurobiology, Barrow Neurologic Institute, Phoenix, Arizona (A.A.G., R.J.L., P.W.); and Centre National de la Recherche Scientifique, Unité Neurobiologie Intégrative des Systèmes Cholinergiques, Institut Pasteur, Paris, France (U.M.)

Received April 22, 2014; accepted July 7, 2014

ABSTRACT

We examined $\alpha_7\beta_2$-nicotinic acetylcholine receptor ($\alpha_7\beta_2$-nAChR) expression in mammalian brain and compared pharmacological profiles of homomeric α_7-nAChRs and $\alpha_7\beta_2$-nAChRs. α-Bungarotoxin affinity purification or immunoprecipitation with anti-α_7 subunit antibodies (Abs) was used to isolate nAChRs containing α_7 subunits from mouse or human brain samples. $\alpha_7\beta_2$-nAChRs were detected in forebrain, but not other tested regions, from both species, based on Western blot analysis of isolates using β_2 subunit–specific Abs. Ab specificity was confirmed in control studies using subunit-null mutant mice or cell lines heterologously expressing specific human nAChR subtypes and subunits. Functional expression in *Xenopus* oocytes of concatenated pentameric $(\alpha_7)_5$-, $(\alpha_7)_4(\beta_2)_1$-, and $(\alpha_7)_3(\beta_2)_2$-nAChRs was confirmed using two-electrode voltage clamp recording of responses to nicotinic ligands. Importantly, pharmacological profiles were indistinguishable for concatenated $(\alpha_7)_5$-nAChRs or for homomeric α_7-nAChRs constituted from unlinked α_7 subunits. Pharmacological profiles were similar for $(\alpha_7)_5$-, $(\alpha_7)_4(\beta_2)_1$-, and $(\alpha_7)_3(\beta_2)_2$-nAChRs except for diminished efficacy of nicotine (normalized to acetylcholine efficacy) at $\alpha_7\beta_2$- versus α_7-nAChRs. This study represents the first direct confirmation of $\alpha_7\beta_2$-nAChR expression in human and mouse forebrain, supporting previous mouse studies that suggested relevance of $\alpha_7\beta_2$-nAChRs in Alzheimer disease etiopathogenesis. These data also indicate that $\alpha_7\beta_2$-nAChR subunit isoforms with different α_7/β_2 subunit ratios have similar pharmacological profiles to each other and to α_7 homopentameric nAChRs. This supports the hypothesis that $\alpha_7\beta_2$-nAChR agonist activation predominantly or entirely reflects binding to α_7/α_7 subunit interface sites.

Introduction

Several nicotinic acetylcholine receptor (nAChR) subtypes are expressed widely along the entire neuraxis and are involved in many of the physiologic functions of the central and peripheral nervous systems (Albuquerque et al., 2009; Hurst et al., 2013). nAChR activity controls important aspects of synaptic function and brain development, including the proliferation and differentiation of neural progenitors, neural migration, and neuronal maturation (Griguoli and Cherubini, 2012; Picciotto et al., 2012; Yakel, 2013). Furthermore, nAChR dysfunction may play an important role in a variety of neurologic diseases, including neurodegenerative and psychiatric diseases (Gotti and Clementi, 2004; Lewis and Picciotto, 2013).

$\alpha_4\beta_2$- and homomeric α_7-nAChRs are the most widely expressed subtypes in mammalian brain. The latter are thought to contain five identical agonist binding sites located at subunit interfaces in extracellular domains (Gotti and Clementi, 2004; Whiteaker et al., 2007). Pharmacological hallmarks of α_7-nAChRs are their high sensitivity to antagonism by snake venom–derived polypeptide toxins such as α-bungarotoxin (α-Bgtx) and α-cobratoxin (α-Cbtx), and their sensitivity to choline [a product of acetylcholine (ACh) hydrolysis] as an agonist (Albuquerque et al., 1997, 2009). α_7-nAChRs are highly expressed in the cortex, hippocampus, and subcortical limbic regions, and (at lower levels) in the thalamus and basal ganglia. α_7-nAChRs that are

This research was supported by the European Union Seventh Framework Programme [Grant HEALTH-F2-2008-20208 (to C.G. and M.Z.)], CNR Research Project on Aging, Regione Lombardia Project NUTEC [Grant 30263049], Italian Ministry of Health [Grant RF2009-1549619 (to M.Z.)], and the National Institutes of Health National Institute on Drug Abuse [Grant R21-DA026627], and Barrow Neurologic Foundation (to P.W.). The Newcastle Brain Tissue Resource is supported by the Research Councils UK Medical Research Council [Grant G0400074], National Institute for Health Research Newcastle Biomedical Research Centre, Newcastle upon Tyne National Health Service Foundation Trust, Newcastle University, and the Alzheimer's Society and Alzheimer's Research Trust [Brains for Dementia Research Project].

M.M., M.Z., and A.A.G. contributed equally to this work; and P.W. and C.G. contributed equally to this work and are joint corresponding authors.

dx.doi.org/10.1124/mol.114.093377.

[S] This article has supplemental material available at molpharm.aspetjournals.org.

ABBREVIATIONS: α-Bgtx, α-bungarotoxin; Ab, antibody; α-Cbtx, α-cobratoxin; ACh, acetylcholine; BSA, bovine serum albumin; CC4, 1,2-bis-*N*-cystinylethane; CYT, intracytoplasmic loop; DHβE, dihydro-β-erythroidine; Epi, epibatidine; KO, subunit-null knock out mutants; MLA, methyllycaconitine; nAChR, nicotinic acetylcholine receptor; TEVC, two-electrode voltage clamp; WT, wild-type.

located on or near nerve terminals are involved in control of neurotransmitter release, whereas α_7-nAChRs on dendrites or soma apposed to cholinergic synaptic endings play roles in classic neurotransmission. In both cases, the high calcium permeability of α_7-nAChRs may also result in altered intracellular signaling and gene transcription (Dajas-Bailador and Wonnacott, 2004; Albuquerque et al., 2009). α_7-nAChRs also may be associated with extrasynaptic volume transmission (Lendvai and Vizi, 2008).

Affinity purification of nAChRs using snake venom α-toxins has been performed from brain tissue of various species. Extracts from whole rat brain appear to be predominantly composed of homomeric α_7-nAChRs (Drisdel and Green, 2000). However, homomeric α_7- and α_8-nAChRs (and heteromeric $\alpha_7\alpha_8$-nAChRs) have been identified in chick central nervous system extracts (Keyser et al., 1993; Gotti et al., 1994). Furthermore, studies using heterologous systems have shown that α_7 subunits can form functional channels when combined with α_5 (Girod et al., 1999), β_2 (Khiroug et al., 2002), β_3 (Palma et al., 1999), or β_4 subunits (Criado et al., 2012). Fluorescently tagged nAChR α_7 and β_2 subunits were recently used to characterize the formation of $\alpha_7\beta_2$-nAChRs, and functional differences between α_7- and $\alpha_7\beta_2$-nAChRs have been suggested (Murray et al., 2012). Coexpression of β_2 and α_7 subunits caused a significant decrease in agonist-evoked whole cell current amplitudes, but this decrease occurs without affecting the concentration-response characteristics of a range of common agonists and antagonists (Murray et al., 2012). Other studies have shown that α_7 and β_2 subunits are coexpressed in rat basal forebrain cholinergic neurons and appear to form heteromeric $\alpha_7\beta_2$-nAChRs with subtly different biophysical and pharmacological properties from those of homomeric α_7-nAChRs (Liu et al., 2009). In addition, interaction of these putative $\alpha_7\beta_2$-nAChRs with oligomeric forms of amyloid-β ($A\beta_{1\text{-}42}$) may be relevant in the etiology of Alzheimer disease (Liu et al., 2013).

These previous studies suggest that the function and pharmacology of α_7*-nAChRs (where the asterisk denotes the known or possible presence of other nAChR subunits than α_7; Lukas et al., 1999) may be more complex than previously thought, and that $\alpha_7\beta_2$-nAChR expression may be restricted to forebrain areas. However, heteromeric α_7*-nAChRs have not yet been directly detected biochemically, nor have they been definitively identified in human brain. We used the α_7-nAChR–selective ligand, α-Bgtx, to affinity purify α_7*-nAChRs from selected brain areas of humans or of wild-type (WT) or β_2 subunit-null mutant (KO) mice. The subunit compositions of these isolated α_7*-nAChRs were analyzed by Western blot analysis using subunit-specific anti-α_7 or anti-β_2 antibodies. The results show expression of $\alpha_7\beta_2$-nAChRs in both WT mouse and human forebrain samples, but not in brains from β_2 KO mice. Moreover, concatemeric (linked subunit) constructs, the *Xenopus* oocyte system, and two-electrode voltage clamp (TEVC) recording were used to confirm functional expression of $\alpha_7\beta_2$-nAChRs. This work defined α_7 and β_2 subunit stoichiometries that enable $\alpha_7\beta_2$-nAChR function and showed similar pharmacological characteristics across α_7- and $\alpha_7\beta_2$-nAChR subtypes. The results confirm commonalities in expression of $\alpha_7\beta_2$-nAChRs in humans and mice, and support hypotheses linking $\alpha_7\beta_2$-nAChRs, cholinergic signaling loss, and roles for $A\beta_{1\text{-}42}$ in etiopathogenesis of at least a subset of human dementias.

Materials and Methods

Animals and Materials

This study used 4- to 6-month-old male, pathogen-free, C57BL/6 WT, α_7 KO, or β_2 KO mice (Picciotto et al., 1995; Orr-Urtreger et al., 1997) obtained from Dr. U. Maskos (Pasteur Institute, Paris, France). All animal experiments were conducted in accordance with the European Community Council Directive (86/609/EEC) of November 24, 1986.

(±)-[^{3}H]epibatidine (Epi; specific activity, 66Ci/mmol) and [^{125}I]-α-Bgtx (specific activity of 200–216 Ci/mmol) were purchased from Perkin Elmer (Waltham, MA). Nonradioactive α-Bgtx, Epi, and nicotine were purchased from Tocris Bioscience (Bristol, UK, or Minneapolis, MN), as were dihydro-β-erythroidine (DHβE), and methyllycaconitine (MLA). Sazetidine-A (also known as AMOP-H-OH) was kindly supplied by Dr. Alan Kozikowski (University of Illinois, Chicago, IL, USA). 1,2-bis-*N*-cytisinylethane (CC4) also was used (Riganti et al., 2005). α-Cbtx and all other reagents were sourced from Sigma-Aldrich (St. Louis, MO) unless otherwise specified.

Human Tissues

Human cerebellum was provided by the Newcastle Brain Tissue Resource on the basis of a collaboration with Dr. Jennifer Court (Newcastle upon Tyne General Hospital, Newcastle upon Tyne, UK). Samples were all collected by the Newcastle Brain Tissue Resource with informed consent and appropriate ethical approval. Case details are shown in Table 1. The approvals and method for categorizing the subjects' smoking status are outlined in the methods section of Court et al. (2005). Human basal forebrain tissue was provided by Dr. Emanuele Sher (Lilly Research Center, Windlesham, Surrey, UK), and was also collected with appropriate informed consent in accordance with all applicable laws and regulations.

Transfected Cells

Human α_2-, α_3-, β_2-, and β_4-nAChR subunit clones in the mammalian expression vector pcDNA3 were gifts from Dr. Sergio Fucile (University of Rome, Rome, Italy). The human α_7-nAChR subunit clone in pcDNA3 was a gift of Dr. Roberta Benfante (CNR Institute of Neuroscience, Milan, Italy). HEK293 and SH-SY5Y cells were transiently transfected using the $Ca_3(PO4)_2$ method or the Jet-PEI reagent (Polyplus, Euroclone, Italy) transfection. For the α_7 plasmid, 1.5×10^6 cells were transfected with 6 μg plasmid using the Jet-PEI. For each of the α_2, α_3, α_4, and β_2 or β_4 subunits, 20 μg plasmids for 1.5×10^6 cells was used, with the $Ca_3(PO4)_2$ method. nAChR expression by cells was analyzed 24 hours after transfection.

Antibody Production and Characterization

We used affinity-purified, subunit-specific polyclonal antibodies (Abs), produced in rabbit against peptides derived from the C-terminal (COOH) or intracytoplasmic loop (CYT) of human or mouse nAChR subunit sequences, as previously described (Gotti et al., 2006; Grady et al., 2009). The Ab against the COOH peptide (SAPNFVEAVSKDFA) was used for α_7 subunits in mouse and human tissues. Abs directed

TABLE 1
Details of cases sampled for receptor analysis
Values are the mean ± S.E.M.

Brain Region	Cases	Age	Postmortem Delay	Male/Female
	n	*yr*	*h*	
Basal forebrain	4	65.7 ± 9.4	2 > 8 2 (2–6)	3/1
Cerebellum smokers	4	73.0 ± 3.9	>8	2/2
Cerebellum nonsmokers	4	68.7 ± 6.6	>8	2/2

There were no significant differences between groups for age.

against the α_7 mouse CYT peptide (PSGDPDLAKILEEVRYIANRFRC) or the human CYT peptide (QMQEADISGYIPNGQMQEADISGYIPNG) were used for mouse and human tissues, respectively. For the β_2 subunit, we used antibodies directed against two different cytoplasmic human β_2 peptides: RQRREREGAGALFFREAPGADSCTY [$\beta_{2(1)}$] and cgIADHMR-SEDDDQSVREDWKYV [$\beta_{2(2)}$].

The specificity of the affinity-purified Abs was tested by immunoprecipitation studies using α_7 WT or α_7 KO hippocampus and β_2 WT or β_2 KO mouse cortex (the results are shown in Supplemental Fig. 1). The same Abs also were tested by means of Western blotting (Supplemental Fig. 1). To exclude any cross-reactivity between nAChR subunits, anti-$\beta_{2(1)}$- or anti-α_7 human subunit Abs were also tested by means of immunoprecipitation studies and Western blotting in HEK293 cells transfected to express human $\alpha_2\beta_4$-, $\alpha_4\beta_2$-, $\alpha_4\beta_4$, or $\alpha_3\beta_4$-nAChR subtypes or in SH-SY5Y cells transfected to express human α_7-nAChRs (see above) (results are shown in Supplemental Fig. 2).

Purification of α-Bgtx–Binding nAChRs

For studies using mice, approximately 100 mg of basal forebrain or hippocampus tissue microdissected from either WT or subunit-null mice were pooled in every experiment. The tissue was homogenized in 10 ml of 50 mM Na phosphate, pH 7.4, 1 M NaCl, 2 mM EDTA, 2 mM EGTA, and 2 mM phenylmethylsufonylfluoride (to covalently inactivate serine protease activity), and the homogenates were diluted and centrifuged for 1.5 hours at 60,000*g*. The entire membrane homogenization, dilution, and centrifugation procedure were then repeated, and the resulting pellets were collected, rapidly rinsed with 50 mM Tris HCl, pH 7, 120 mM NaCl, 5 mM KCl, 1 mM $MgCl_2$, 2.5 mM $CaCl_2$, and 2 mM phenylmethylsufonylfluoride. The washed pellets were then resuspended in 2 ml of the same buffer, further supplemented with 20 μg/ml of each of the following protease inhibitors: leupeptin, bestatin, pepstatin A, and aprotinin. Triton X-100 at a final concentration of 2% was added to the washed membranes, which were extracted for 2 hours at 4°C. The extracts were centrifuged for 1.5 hours at 60,000*g*, recovered, and an aliquot of the supernatants was collected for protein measurement using the BCA protein assay (Pierce Biotechnology, Rockford, IL), with bovine serum albumin (BSA) as the standard. Extracts (2 ml) were incubated with 200 μl Sepharose–α-Bgtx (concentration of coupled toxin 1 mg/ml of gel) and shaken overnight at 4°C. The following day, the beads were centrifuged, the supernatant was recovered, and the resins were washed 4–6 times by resuspension followed by centrifugation. After washing, the Sepharose–α-Bgtx beads with bound nAChRs (purified α-Bgtx–binding receptors) were incubated with one to two volumes of Laemmli sample buffer (125 mM Tris phosphate, 4% SDS, 20% glycerol, 0,02% bromophenol blue, and 10% 2-mercaptoethanol, pH 6.8) and boiled for 2 minutes. The supernatant was then recovered by centrifugation.

In the case of human tissue, α-Bgtx–binding sites were purified using the same procedure as that used for mouse tissue, starting from 600 mg of tissue (see Table 1 for subject details).

Binding Studies

[^{125}I]-α-Bgtx. The binding of [^{125}I]-α-Bgtx to 2% Triton X-100 extracts of mouse tissues was determined by collection onto DEAE-Sepharose Fast Flow (GE Healthcare, Uppsala, Sweden). Triton extracts (250 μl) from each experimental group were incubated overnight with a saturating concentration (5 nM) of [^{125}I]-α-Bgtx at 20°C in the presence of 2 mg/ml BSA. Specific radioligand binding was defined as total binding minus the nonspecific binding determined in the presence of 1 μM unlabeled α-Bgtx. Nonspecific binding averaged 30–40% of total binding. Binding to α_7*-nAChRs could also be measured in an immunoprecipitation assay format. Receptor extracts were labeled with [^{125}I]-α-Bgtx (5 nM in the presence or absence of 1 μM unlabeled α-Bgtx to define total and nonspecific binding). The labeled extract could then be bound to protein A beads via anti-α_7 subunit Abs (described later in the *Materials and Methods*). Similar amounts of specific binding were recorded in either assay format, and nonspecific binding was between 10 and 15% of total binding.

[^{3}H]Epi. Binding of [^{3}H]Epi to nAChRs in 2% Triton X-100 brain tissue extracts obtained was also assessed. [^{3}H]Epi binds to multiple heteromeric nAChR subtypes with picomolar affinity and to α_7-nAChR with nanomolar affinity. To ensure that the α_7 nAChR did not contribute to [^{3}H]Epi binding, in solubilized extracts, binding was performed in the presence of 1 μM α-Bgtx, which specifically binds to α_7-nAChRs (and thus prevents [^{3}H]Epi binding to these sites).

As for [^{125}I]-α-Bgtx binding assays, binding sites were captured using DEAE-Sepharose Fast Flow, after overnight incubation of 250-μl aliquots of the extracts with 1 nM [^{3}H]Epi at 4°C. Nonspecific binding (averaging 5–10% of total binding) was determined in parallel samples containing 100 nM unlabeled Epi.

Immunoprecipitation

For immunoprecipitation studies of heteromeric receptors present in human tissues, we used Abs specific for α_2, α_3, α_4, α_5, β_2, or β_4 subunits directed against human subunit peptides as previously described (Gotti et al., 2006). For α_6 and β_3 subunits, we used Abs directed against peptides of mouse subunit sequences, also as previously characterized and described (Grady et al., 2009). The immunoprecipitation capacities of the anti-human subunit Abs ranged from 90 to 100% of the [^{3}H]Epi–labeled receptors (mean of three independent experiments). For immunoprecipitation experiments, affinity-purified Abs were covalently immobilized on agarose-Protein A beads at a concentration of 4 mg/ml wet resin. Immunoprecipitation was then performed by adding 20 μl agarose-Protein A beads with bound, affinity-purified Abs to 200 μl of 1 nM [^{3}H]Epi–labeled extracts. After overnight incubation, immunoprecipitates were recovered by centrifugation and washed three times with phosphate-buffered saline containing 0.1% Triton X-100.

Immunoblotting and Densitometric Quantification of Western Blot Bands

nAChR subunit contents of tissue extracts or of α-Bgtx–binding complexes were analyzed by Western blotting. For the extracts loaded before and after the purification, 10 μg of proteins were loaded, whereas for the α-Bgtx–purified receptors a constant volume (40 μl), that depending on the tissue, may represent 1/10 or 1/20 of the total recovered Laemmli sample buffer-eluted receptors was loaded onto a 9% acrylamide (Bio-Rad, Hercules, CA) gel and subjected to SDS-PAGE. After SDS-PAGE, proteins were electrophoretically transferred to nitrocellulose membranes with 0.45-mm diameter pores (Schleicher and Schuell, Dassel, Germany). The blots were blocked overnight in 5% nonfat milk in Tris-buffered saline, washed in a buffer containing 5% nonfat milk and 0.3% Tween 20 in Tris-buffered saline, incubated for 2 hours with the primary antibody (1–2.5 mg/ml), and then incubated with the appropriate peroxidase-conjugated secondary Abs (Sigma-Aldrich). After 10 washes, peroxidase was detected using a chemiluminescent substrate (Pierce Biotechnology). The signal intensity of the Western blot bands was measured using an Epson 4500 gel scanner. The developed films were scanned as a TIFF image in eight-bit grayscale format at a resolution setting of 300 dpi. All of the films obtained from the separate experiments were acquired in the same way and scanned in parallel with a calibrated optical density step tablet from Stouffer (Stouffer Graphics Arts, Mishawaka, IN).

The images were analyzed using ImageJ software (National Institutes of Health, Bethesda, MD) (Schneider et al., 2012). The pixel values of the images were transformed to optical density values by the program using the calibration curve obtained by acquiring the calibrated tablet with the same parameters as those used for the images. The immunoreactive bands were quantified in four separate experiments for the mouse hippocampus and basal forebrain as previously described (Grady et al., 2009)

Concatemeric α_7*-nAChR Constructs

Fully pentameric nAChR concatemers were constructed from human nAChR subunit sequences. cDNAs encoding concatemers were created using the same subunit layout we have previously employed to encode high- and low-agonist-sensitivity $\alpha_4\beta_2$*-nAChR isoforms and $\alpha_3\beta_4(\alpha_5$[D/N])-nAChRs (George et al., 2012; Eaton et al., 2014). Subunits were arranged in the order α_7-α_7-α_7-α_7-α_7 (α_7 homopentamer), α_7-α_7-β_2-α_7-α_7, or α_7-β_2-α_7-β_2-α_7. Kozac and signal peptide sequences were removed from all subunit sequences with the exception of subunits expressed in the first position of the concatamer. Subunits were linked by alanine-glycine-serine repeats designed to provide a complete linker length (including the C-terminal tail of the preceding subunit) of 40 ± 2 amino acids. At the nucleotide level, linker sequences were designed to contain unique restriction sites that allow easy removal and replacement of individual α_7 and β_2 subunits. The protein sequences for the human nAChR subunits were encoded by synthetic nucleotide sequences optimized for expression systems (GeneArt; Life Technologies, Grand Island, NY). Optimization included minimization of high GC content sequence segments, improved codon usage, reduction of predicted RNA secondary structure formation, and removal of sequence repeats and possible alternative start and splice sites. Sequences of all subunits, together with their associated partial linkers, were confirmed by DNA sequencing (GeneArt). Each concatamer was subcloned into the pSGEM oocyte high-expression vector (from Dr. Michael Hollmann, Ruhr-Universitaet, Bochum, Germany). For comparison, homomeric α_7-nAChRs were also expressed from unlinked individual subunits (cDNA clone also synthesized and optimized by GeneArt). The unlinked human α_7 subunit cDNA was also subcloned into the pSGEM vector.

RNA Synthesis

Plasmids containing concatemeric α_7-homopentameric or $\alpha_7\beta_2$-nAChR constructs, or individual α_7-nAChR subunits, were linearized with NheI (2 hours at 37°C), and the reaction mix was treated with proteinase K (30 minutes at 50°C). cRNAs were transcribed using the mMessage mMachine T7 kit (Applied Biosystems/Ambion, Austin, TX). Reactions were treated with TURBO DNase (1 U for 15 minutes at 37°C) and cRNAs were purified using the Qiagen RNeasy Clean-Up kit (Qiagen, Valencia, CA). cRNA purity was confirmed on a 1% agarose gel and preparations were stored at −80°C.

Xenopus Oocytes and RNA injection

Xenopus oocytes were purchased from Ecocyte Bioscience US (Austin, TX) and incubated upon arrival at 13°C. The tips of pulled glass micropipettes were broken to achieve an outer diameter of approximately 40 μm (resistance of 2–6 MΩ), and pipettes were used to inject 20–60 nl containing 10 ng of cRNA/oocyte. To improve functional expression of α_7*-nAChRs, Ric-3 mRNA was also coinjected (Halevi et al., 2002). A ratio of 1:50 Ric-3/α_7 subunit mRNA by mass was determined to be optimally effective in pilot experiments (data not shown).

TEVC Recording of α_7- and $\alpha_7\beta_2$-nAChR Function

TEVC recordings were made at room temperature (20°C) in oocyte saline solution (containing 82.5 mM NaCl, 2.5 mM KCl, 5 mM HEPES, 1.8 mM $CaCl_2{\cdot}_2H_2O$, and 1 mM $MgCl_2{\cdot}_6H_2O$, pH 7.4). Seven to 14 days after injection, *Xenopus* oocytes expressing concatenated α_7*-nAChRs were voltage clamped at −70 mV with an Axoclamp 900A amplifier (Molecular Devices, Sunnyvale, CA). Recordings were sampled at 10 kHz (low-pass Bessel filter, 40 Hz; high-pass filter, DC), and the resulting traces were saved to disk (Clampex v10.2; Molecular Devices). Data from oocytes with leak currents (I_{leak}) > 50 nA were excluded from recordings.

Nicotinic Receptor Pharmacology

Fresh stock drug solutions (agonists: ACh, choline, nicotine, sazetidine, and CC4; antagonists: DHβE, MLA, mecamylamine, and α-Cbtx) were made daily and diluted as required. Agonists and antagonists were applied using a 16-channel, gravity-fed perfusion system with automated valve control (AutoMate Scientific, Inc.; Berkeley, CA). All solutions were supplemented with atropine sulfate (1.5 μM) to ensure that muscarinic ACh receptor responses were blocked and thus not recorded. Oocytes expressing loose subunits and/or concatemeric α_7- or $\alpha_7\beta_2$-nAChRs were perfused with nAChR agonists for 5 seconds with 60-second washout times between each subsequent application. Oocytes were preincubated with nAChR antagonists for 2 minutes prior to activation with ACh (10 mM; 5 seconds). For experiments using α-Cbtx, bath and drug solutions were supplemented with 0.1% BSA to reduce loss of this peptide ligand by adsorption to the TEVC apparatus.

Data Analysis

The expression of [^{3}H]Epi and [^{125}I]-α-Bgtx receptors and the subunit contents of the [^{3}H]Epi receptors expressed in the mouse and human samples were statistically compared using unpaired *t* tests. In human cerebellum samples from smokers and nonsmokers, results were compared using an unpaired *t* test. Statistical analyses were performed using GraphPad Prism 5.0 software (GraphPad Software, Inc., La Jolla, CA).

For TEVC data, EC_{50} and IC_{50} values were determined from nAChR-mediated peak currents through nonlinear least-squares curve fitting (GraphPad Prism 5.0) using unconstrained, monophasic logistic equations to fit all parameters, including Hill slopes. Desensitization/inactivation of α_7*-nAChR currents in the presence of 10 mM (maximally stimulating) ACh was also analyzed by nonlinear least-squares curve fitting in Graph Pad Prism 5.0. These data were best fit by a two-phase exponential decay equation. One-way analysis of variance was used to compare parameters between multiple groups in each case. The Tukey multiple comparison test was used for post hoc analysis to compare the means of three or more groups (GraphPad Prism 5.0).

Results

α-Bgtx–Binding Sites in WT or β_2 KO Mice

In preliminary experiments, we analyzed nAChR expression in 2% Triton X-100 extracts obtained from the hippocampus or basal forebrain of WT or β_2 KO mice (Table 2). By two different approaches (immunoprecipitating [^{125}I]-α-Bgtx–labeled receptors using anti-α_7 subunit Abs and by [^{125}I]-α-Bgtx binding to Triton extracts), we determined that the density of α_7*-nAChRs in the mouse hippocampus is more than two times higher than that in the murine basal forebrain. During α-Bgtx binding site purification, we determined that 85–95% of those sites in Triton X-100 extracts were bound by α-Bgtx–Sepharose 4B affinity resins, whereas more than 95% of high-affinity [^{3}H]Epi binding was recovered in the flow-through.

The densities of [^{3}H]Epi–binding nAChRs were similar between the two regions (Table 2). Elimination of β_2 subunit expression dramatically reduced expression of [^{3}H]Epi–binding nAChRs in both regions, indicating that this binding is almost entirely due to β_2*-nAChRs. By contrast, [^{125}I]-α-Bgtx (α_7*-nAChR) expression was not significantly different between WT and β_2 KO mice in either the hippocampus or basal forebrain.

In addition, Western blot analysis was performed on α-Bgtx binding sites affinity purified from the hippocampus of WT or β_2 KO mice and probed with anti-α_7 (top) or anti-β_2 (bottom) subunit Abs (Fig. 1A). Confirming results from the binding studies, Western blots also showed no significant differences in presumed α_7*-nAChR levels (i.e., polypeptide labeled with

TABLE 2
Levels of [^{3}H]Epi and [^{125}I]α-Bgtx binding to 2% Triton X-100 extracts in two different brain areas of WT and β_2 KO mice
Values are the mean ± S.E.M. from three separate experiments.

Brain Region	[^{3}H]Epi	[^{125}I]-αBgtx
	fmol/mg protein	
β_2 WT Hippocampus	36.3 ± 2.3	37.7 ± 2.3
β_2 KO Hippocampus	1.0 ± 0.3*	39.9 ± 1.0
β_2 WT Basal forebrain	44.5 ± 3.5	15.2 ± 2.5
β_2 KO Basal forebrain	0.5 ± 0.2*	15.1 ± 2.6

*$P < 0.001$ (significantly different from $\beta_2^{+/+}$ by t test).

anti-α_7 subunit Abs) in whole extracts from WT or β_2 KO mouse hippocampus (lane 1 in top two panels). Moreover, affinity purification on α-Bgtx affinity resins isolated comparable levels of α_7*-nAChRs from WT or β_2 KO mouse hippocampus (compare lanes 1 and 3 of Fig. 1A top) but did not isolate nAChRs containing β_2 subunits (compare lanes 1 and 3 of Fig. 1A, bottom left), which instead were found in the flow-through fraction (lane 2; Fig. 1A, bottom left). As expected, no β_2*-nAChRs were found in extracts isolated on Bgtx resins or in the flow-through from that separation for tissue taken from β_2 KO mice (Fig. 1A, lower right panel lanes 1–3).

In further agreement with the findings of the binding studies, Western blot analysis showed that basal forebrain extracts contained fewer α_7*-nAChRs (i.e., immunoreactive α_7 protein) than hippocampal extracts, whereas amounts of immunoreactive β_2 subunits were very similar across brain regions. Analysis of the Western blots probed using anti-β_2 subunit Abs showed clearly detectable β_2 subunit presence in α_7*nAChRs isolated on Bgtx resins from tissue derived from basal forebrain, but not from the hippocampus (compare lanes 3 of the bottom-left panels of Fig. 1, A and B). The percentage of β_2 subunit present in the α-Bgtx purified receptor was determined by western blotting by loading on the same gel 10 μg of 2% Triton extract and 1/10 of the α-Bgtx purified receptor. We found that the immunoreactivity of the β_2 subunit determined in the purified α-Bgtx was 2.25% ± 0.6% ($n = 4$) of the total β_2 subunit immunoreactivity measured in the basal forebrain extracts of WT mice.

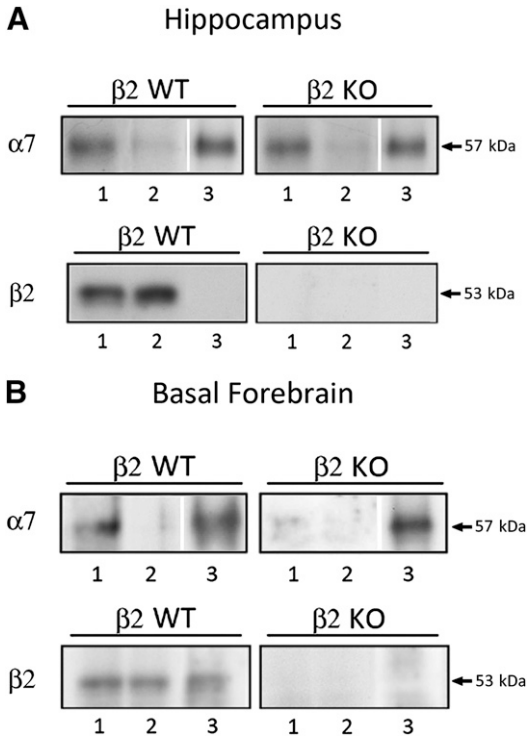

Fig. 1. Western blot analysis of nAChR subunit content in α-Bgtx–purified receptors prepared from 2% Triton X-100 extracts of WT and β_2 KO mouse hippocampi (A) and basal forebrain samples (B). (A) α-Bgtx–purified receptors were prepared from mouse hippocampi by incubating extracts with Sepharose 4B covalently bound with α-Bgtx. The bound receptors were recovered from the beads using Laemmli sample buffer. Western blot analysis of 10 μg 2% Triton X-100 extracts of the hippocampus before (lane 1) and after α-Bgtx purification (lane 2; supernatant), and 1/20 of the corresponding α-Bgtx purified receptors (lane 3; recovered from beads). The blots were probed with an anti-α_7 Ab (top) or β_2(1) Ab (bottom). (B) α-Bgtx–purified receptors were prepared as described above. Western blot analysis of 10 μg 2% Triton X-100 extracts of the basal forebrain before (lane 1) and after α-Bgtx purification (lane 2; supernatant), and 1/10 of the corresponding α-Bgtx–purified receptors (lane 3; recovered from beads). The blots were probed with an anti-α_7 Ab (top) or β_2(1) Ab (bottom).

α-Bgtx–Binding Sites in Human Brain

The possible presence of $\alpha_7\beta_2$-nAChRs in human brain was analyzed using post mortem samples of basal forebrain and cerebellum. In preliminary experiments, we characterized nAChR subtypes expressed in basal forebrain and cerebellum and their levels in 2% Triton extracts (Table 3). The average level of [^{125}I]-α-Bgtx–labeled (α_7*)-nAChRs was higher in basal forebrain than cerebellum.

The level of [^{3}H]Epi–binding nAChRs in cerebellum depended on smoking status. As shown in Table 3, the density of non-α_7*-nAChRs measured by means of [^{3}H]Epi binding was higher in smokers than in nonsmokers ($P = 0.02$). Based on immunoprecipitation using subunit-specific Abs, in both tissues the large majority of [^{3}H]Epi–binding sites contained the β_2 subunit associated with the α_4 subunit ($\alpha_4\beta_2$-nAChR: 75% in basal forebrain and 60 and 67% in cerebellum of smokers and nonsmokers, respectively). An additional 14% of [^{3}H]Epi–binding sites in the basal forebrain were $\alpha_2\beta_2$*-nAChRs, whereas this subtype accounted for only 7% of cerebellar [^{3}H]Epi–binding sites. The largest region-to-region difference was for $\alpha_3\beta_2$*-nAChRs: Whereas those sites accounted for 4.8% of [^{3}H]Epi–binding sites in the basal forebrain, they represented 32% in the cerebellum.

α-Bgtx affinity-purified binding sites were obtained from three human basal forebrain (Fig. 2, lanes 1–3) or three human cerebellum (Fig. 2, lanes 5–7) samples. These sites were Western blotted and probed with anti-α_7 subunit Abs (top) or two different anti-β_2 subunit Abs [anti-$\beta_{2(1)}$ Abs,

TABLE 3
Levels of [^{3}H]Epi and [^{125}I] α-Bungarotoxin binding to 2% Triton X-100 extracts in the two different human brain regions
Values are the mean ± S.E.M. of the four samples in each group.

Brain Region	[^{3}H]Epi	[^{125}I]-α-Bgtx
	fmol/mg protein	
Basal forebrain	31.8 ± 8.5	80.7 ± 7.0
Cerebellum nonsmokers	22.5 ± 2.6	45.7 ± 5.1
Cerebellum smokers	39.7 ± 5.3*	48.3 ± 6.5

*$P = 0.02$ (significant differences in cerebellar membrane [^{3}H]Epi binding between smokers and nonsmokers: unpaired t test). No significant difference was seen between [^{125}I]-α-Bgtx binding levels in cerebellar samples taken from smokers versus nonsmokers, by the same measure.

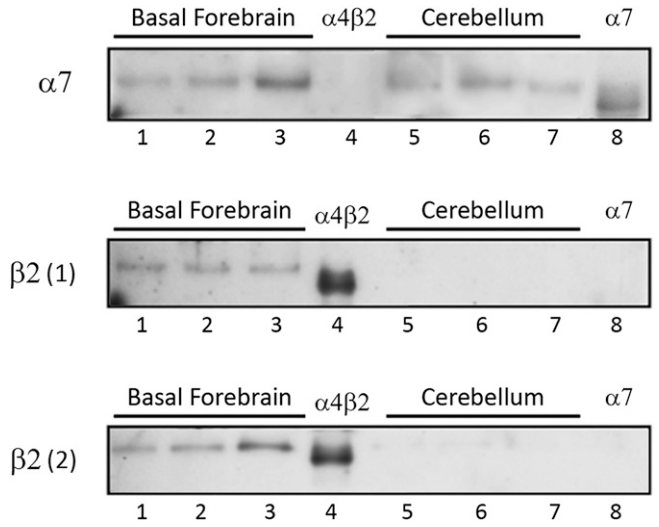

Fig. 2. Western blot analysis of α-Bgtx–purified nAChRs prepared from human basal forebrain and cerebellum. α-Bgtx–binding nAChRs were purified from the same volume of 2% Triton X-100 extracts of basal forebrain and cerebellum by incubating them with Sepharose 4B covalently bound with α-Bgtx. The bound receptors were eluted using sample buffer and an identical volume of purified receptors was loaded on the gel. The Western blots were probed with anti-α_7 Ab (top) or anti-β_2 Ab (bottom).

middle; and anti-$\beta_{2(2)}$, bottom] targeting different epitopes within the β_2 subunit. Control samples were extracts from $\alpha_4\beta_2$-nAChR–expressing transfected HEK cells (lane 4) or from α_7-nAChR–expressing transfected SH-SY5Y cells (lane 8), also probed with the Abs. Levels of immunoreactivity for the α_7 subunit were very similar in samples loaded in lanes 1, 2, 5, and 6, higher in the sample loaded in lane 3, and lower in the sample loaded in lane 7. Similar isolates from HEK-$\alpha_4\beta_2$ cells were negative but SH-SY5Y-α_7 cells contained immunoreactive α_7 subunits (Fig. 2, upper panel, lanes 4 and 8, respectively). Isolation of α-Bgtx binding sites also yielded anti-β_2 subunit Ab-labeled proteins from basal forebrain samples but not from the cerebellum, regardless of whether the cerebellum samples were obtained from smokers or nonsmokers. Such immunoreactivity was absent in extracts from SH-SY5Y-α_7 cells but very evident in HEK-$\alpha_4\beta_2$ cells (Fig. 2, middle and lower panels, lanes 8 and 4, respectively). Both the α_7 and β_2 subunits present in the human tissues show a slightly higher molecular weight then the corresponding transfected subunits. This is probably due to differences in glycosylation between native and transfected receptors.

Since it has been shown in a heterologous expression system that an $\alpha_7\beta_4$-nAChR subtype may be formed (Criado et al., 2012), we also probed human α-Bgtx–purified sites with anti-β_4 subunit Abs with proven specificity (Supplemental Fig. 2, bottom). No specific labeling was observed in either the human basal forebrain or cerebellum samples, showing absence of $\alpha_7\beta_4$-nAChRs. Collectively, these results clearly indicate that $\alpha_7\beta_2$-nAChRs are present in the human basal forebrain but not in the cerebellum.

Functional Expression of Concatemeric α_7*-nAChRs from Human Subunits

Heterologous expression has shown assembly of functional $\alpha_7\beta_2$*-nAChRs (see the *Introduction*), but the way(s) in which α_7 and β_2 subunits might combine from individual, unlinked, subunits could not be defined. Accordingly, we used a linked-subunit approach to produce α_7*-nAChRs with defined subunit ratios and assembly orders. Each of the three concatemeric constructs [$(\alpha_7)_5$-nAChR homopentamer, $(\alpha_7)_4(\beta_2)_1$-nAChR, and $(\alpha_7)_3(\beta_2)_2$-nAChR] showed concentration-dependent ACh-evoked function (representative traces shown in Fig. 3, A–D). This function, although smaller than that measured in *Xenopus* oocytes expressing homomeric α_7-nAChRs from unlinked human α_7 subunits (typically $>$ 1 μA at 7 days after mRNA injection) was easily measurable (approximately 100–300 nA peak current response, depending on the construct). The time course of desensitization/inactivation after a peak response stimulated by 10 mM ACh (maximally stimulating concentration) was also measured for each construct. For each construct, desensitization/inactivation was best fit by a double-exponential decay model. As detailed in the legend to Fig. 3, no significant differences were seen between the fast desensitization/inactivation time constants calculated for each group. This is not surprising since the apparent time constants will likely reflect the relatively slow kinetics of agonist application in the apparatus, rather than the much faster kinetics of α_7*-nAChR desensitization (Papke, 2010). Indeed, the apparent τ_{fast} values are very similar to those measured for solution exchange in our apparatus (Eaton et al., 2014). However, the τ_{slow} value calculated for the $(\alpha_7)_3(\beta_2)_2$ construct was significantly slower than those associated with the other groups. Thus, despite the admitted disadvantages of measuring kinetic parameters in the *Xenopus* oocyte expression system, there is some evidence that $\alpha_7\beta_2$*-nAChR desensitization may be slower than that of homomeric α_7-nAChRs.

Agonist and Antagonist Pharmacology of Concatemeric Human α_7*-nAChRs

Pharmacological parameters of selected ligands were determined at concatenated α_7*-nAChRs. Compounds chosen included the prototypical agonists, ACh and nicotine, choline (which is a relatively selective agonist of α_7-nAChR; Alkondon et al., 1997), and two further agonists with established selectivity for other β_2*-nAChR subtypes (sazetidine-A and CC4; Xiao et al., 2006; Kozikowski et al., 2009; Sala et al., 2013). Agonist pharmacological profiles for $(\alpha_7)_5$-, $(\alpha_7)_4(\beta_2)_1$-, and $(\alpha_7)_3(\beta_2)_2$-nAChR subtypes were largely indistinguishable from each other, and from that for nonconcatemeric (loose-subunit), homomeric α_7nAChRs (Fig. 4; Table 4). The only exception is that nicotine has significantly lower efficacy (normalized to that of ACh) at both $\alpha_7\beta_2$*-nAChR subtypes than at concatemeric $(\alpha_7)_5$-nAChRs or unlinked α_7- nAChRs (which are statistically indistinguishable on this measure). There was also a trend toward lower nicotine potency across all concatemeric α_7*-nAChR constructs, but this did not reach statistical significance (see Table 4). The observed slight trend toward lower choline efficacy, although not significant, is suggestive of the previous observation of 50–70% efficacy of choline versus ACh at putative $\alpha_7\beta_2$-nAChRs expressed from nonlinked subunits (Khiroug et al., 2002; Zwart et al., 2014). Strikingly, both sazetidine-A and CC4 were very weak agonists ($<$10% efficacy normalized to that of ACh) at all α_7*-nAChR subtypes tested, including both $\alpha_7\beta_2$-nAChRs, making it impossible to reliably calculate EC_{50} or Hill slope values from the resulting concentration-response data.

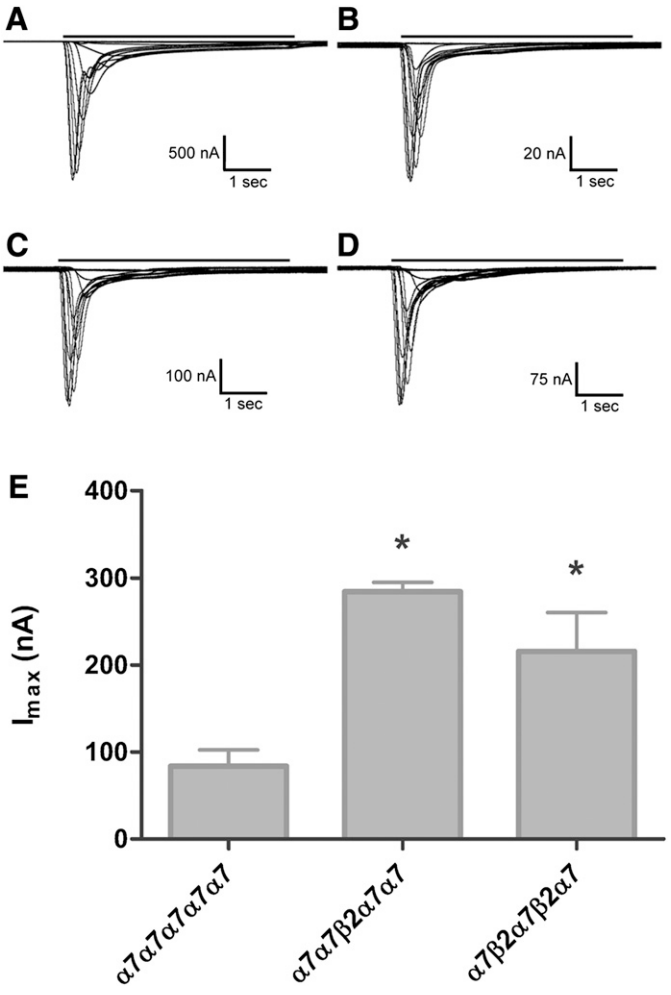

Fig. 3. Representative traces and maximum function (I_{max}) comparison for α_7*-nAChR pentameric concatemer constructs. Oocytes were injected with mRNA encoding unlinked α_7-nAChR subunit monomers (A), concatenated α_7 homopentamers (B), $\alpha_7\beta_2$-nAChRs with the β_2 subunit in position 3 (C), or $\alpha_7\beta_2$-nAChRs with the β_2 subunit in positions 2 and 4 (D). Representative TEVC recordings are shown in each case for ACh concentration-response determinations (see *Materials and Methods* for details). Black bars above each trace represent 5-second applications of ACh at a range of concentrations. The time course of receptor desensitization/inactivation during stimulation with a maximally effective dose of ACh (10 mM) was also investigated for each nAChR construct using additional groups of oocytes. In each case, the time course was best fit by a double-exponential decay. The fast time constants (τ_{fast}) for desensitization/inactivation were statistically indistinguishable by one-way ANOVA across all four groups (unlinked α_7, 436 ± 85 milliseconds; α_7-only concatemer, 214 ± 80 milliseconds; $\alpha_7\beta_2$(p3), 312 ± 55 milliseconds; $\alpha_7\beta_2$(p2,4), 247 ± 35 milliseconds; $F_{[3,11]} = 2.06$, $P = 0.16$; and $n = 3$ in each group). By contrast, the slow time constant (τ_{slow}) for desensitization/inactivation of the $\alpha_7\beta_2$(p2,4) construct was significantly longer that of the other groups. No other differences were detected by a Tukey post hoc comparison ($P < 0.05$). Values were as follows: unlinked α_7, 5109 ± 800 milliseconds; α_7-only concatemer, 3130 ± 585 milliseconds; $\alpha_7\beta_2$(p3), 5073 ± 638 milliseconds; $\alpha_7\beta_2$(p2,4), 6318 ± 365 millisecond; $F_{[3,11]} = 5.29$, $P = 0.02$; and $n = 3$ in each group. (E) Summary of maximal function (I_{max}) measured in each concatemeric nAChR group by stimulation with the full agonist ACh (10 mM). Bars represent mean ± S.E.M. ($n = 3$). I_{max} values were as follows: α_7 only, 83.9 ± 18.6 nA; $\alpha_7\beta_2$(p3), 285 ± 11 nA; and $\alpha_7\beta_2$(p2,4), 216 ± 45 nA. Analysis using one-way ANOVA with a Tukey post hoc comparison showed that incorporation of β_2 subunits resulted in a statistically significant increase in I_{max} ($F_{[2,6]} = 12.7$, $P = 0.007$; denoted by the asterisk). The I_{max} values obtained from the two $\alpha_7\beta_2$-nAChR constructs were statistically indistinguishable from each other. ANOVA, analysis of variance.

Concentration-response relationships were also explored for archetypal α_7 antagonists (MLA and the snake venom α-toxin, α-Cbtx), together with the β_2-selective antagonist DHβE and the noncompetitive antagonist mecamylamine (Fig. 5). The resulting pharmacological parameters are summarized in Table 5. Similar to the agonist pharmacology, antagonist responses were statistically indistinguishable between the α_7* subtypes (including between α_7-only nAChRs expressed from either unlinked subunits, or from the concatenated α_7 homopentameric construct).

Discussion

This study provides the first direct evidence that $\alpha_7\beta_2$-nAChRs are expressed in the mammalian central nervous system. This is demonstrated by isolation of Bgtx-binding or α_7 subunit–containing complexes also shown to contain β_2 subunits from human or mouse forebrain samples. In addition, we have demonstrated for the first time that multiple human $\alpha_7\beta_2$-nAChR isoforms of defined subunit composition have pharmacological profiles similar to each other and to homopentameric α_7-nAChRs.

Our findings indicate that $\alpha_7\beta_2$-nAChRs are found in post mortem, human basal forebrain but not in the cerebellum. Note that total amounts of α_7*-nAChRs are <2-fold different in the two brain regions. Specificity of the anti-α_7 or anti-β_2 Abs used in Western blot analysis of these nAChRs is demonstrated by control studies using cell lines transfected with specific nAChR subunits, and by studies using WT and subunit-null mice. We also found $\alpha_7\beta_2$-nAChR expression in mouse basal forebrain but not hippocampus. Our results agree with earlier findings of $\alpha_7\beta_2$-nAChR expression in mouse basal forebrain (Liu et al., 2009) but not with the same investigators' study in mouse hippocampus (Liu et al., 2012). There could be several explanations for these seemingly discrepant observations. nAChR α_7 and β_2 subunit mRNAs are coexpressed in both basal forebrain and hippocampal cholinergic neurons (Azam et al., 2003). However, fewer than 3% of β_2*-nAChRs in WT mouse basal forebrain extracts (this study) were associated with the α_7 subunit. This indicates that the large majority of α-Bgtx–binding sites are homomeric α_7-nAChRs. Accordingly, we feel that the most likely explanation for the lack of an immunochemically detectable $\alpha_7\beta_2$-nAChR in mouse hippocampus is that it is even less prevalent than in basal forebrain. The previous electrophysiology experiments (Liu et al., 2012) used brain slices from very young mice, whereas our work used tissue from 4- to 6-month-old mice. Therefore, it is also possible that mouse hippocampal $\alpha_7\beta_2$-nAChR expression levels fall from early life into adulthood. Multiple examples of developmental modulation of nAChR subunit expression (including of α_7) have previously been seen (Zoli et al., 1995; Conroy and Berg, 1998; Zhang et al., 1998; Balestra et al., 2000; Flora et al., 2000).

The use of a linked-subunit approach allowed us, for the first time, to directly assess the effects of defined β_2-nAChR subunit incorporation on α_7*-nAChR function. Of critical importance, no significant differences in EC/IC_{50} values or efficacy relative to ACh were seen between concatenated or unlinked-subunit homomeric α_7-nAChRs. This indicates that, as has previously been shown for $\alpha_3\beta_4$*-nAChR (George et al., 2012; Stokes and Papke, 2012), $\alpha_4\beta_2$-nAChR (Zhou et al., 2003; Carbone et al., 2009; Mazzaferro et al., 2011; Eaton

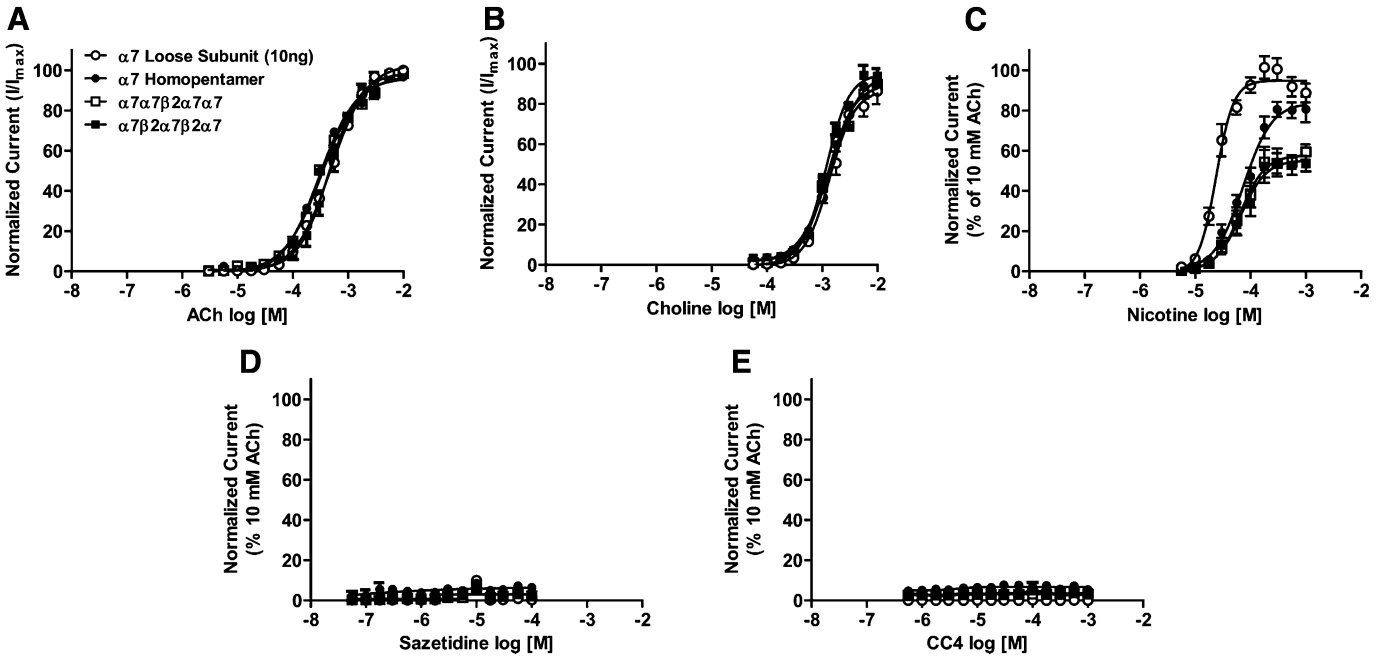

Fig. 4. Agonist concentration-response profiles for α_7- and $\alpha_7\beta_2$-nAChRs. Oocytes were injected with mRNA encoding unlinked α_7 subunits (○), concatenated α_7 homopentamers (●), or concatenated $\alpha_7\beta_2$ pentameric concatemers (□ indicates $\alpha_7\beta_2$-nAChR with the β_2 subunit in position 3; ■ indicates $\alpha_7\beta_2$-nAChR with the β_2 subunit in positions 2 and 4). Oocytes were perfused with the following nAChR agonists: ACh ($10^{-5.5}$ to 10^{-2}; $n = 6$) (A), choline ($10^{-4.25}$ to 10^{-2}; $n = 3$) (B), nicotine ($10^{-5.5}$ to 10^{-3}; $n = 3$) (C), sazetidine-A ($10^{-7.5}$ to 10^{-4}; $n = 3$) (D), or CC4 ($10^{-6.5}$ to 10^{-3}; $n = 3$) (E). All responses within each group were normalized to an initial control stimulation with 10 mM ACh. Data points represent the mean ± S.E.M. Drug potency and efficacy parameters were calculated by nonlinear least-squares curve fitting to the Hill equation (see *Materials and Methods*). The resulting pharmacological parameters and statistical analyses are summarized in Table 4.

et al., 2014), and $\alpha_6\beta_2$*-nAChR (Kuryatov and Lindstrom, 2011) subtypes, introduction of appropriately sized linkers can be performed without altering nAChR functional pharmacology. Several of these previous studies also showed that concatemeric constructs were assembled correctly. To further confirm correct that concatemers were being assembled correctly and not fragmenting and rearranging into unanticipated functional forms, we also coinjected unlinked β_2 subunits containing a gain-of-function mutation (L9'S) in the second transmembrane domain. This additional control has previously been used by us and others (Carbone et al., 2009; Eaton et al., 2014). If concatemer fragments were contributing to the functional nAChR population, the β_2-gain-of-function subunit would assemble into resulting α_7*-nAChR as previously shown (Khiroug et al., 2002; Murray et al., 2012; Zwart et al., 2014). Therefore, if fragments containing α_7 were present, this would result in appearance of a novel $\alpha_7\beta_2$-gain-of-function population with distinctive (more agonist-sensitive) properties. No such effect was seen.

It is noted, however, that overall function was reduced when α_7-nAChR homopentamers were expressed from a concatemeric construct as opposed to unlinked subunits. This relative diminution in function of concatenated nAChR constructs has been noted in the previous publications cited above and appears to be a regular feature of using concatemeric nAChR constructs. Importantly, both $(\alpha_7)_4(\beta_2)_1$-and $(\alpha_7)_3(\beta_2)_2$-nAChR concatemeric constructs expressed more function than did the $(\alpha_7)_5$-nAChR concatemer. This is the opposite of the situation in which loose β_2-nAChR subunits are coexpressed with α_7 subunits (Murray et al., 2012) and replicates an earlier finding in which coexpression of unlinked α_5, α_3, and β_4 nAChR subunits reduced function compared with expression of loose α_3 and β_4 subunits alone, but incorporation of the α_5 subunit into a concatemeric construct actually increased observed function of an $\alpha_3\beta_4$*-nAChR pentameric concatemer (George et al., 2012). As in the previous publication, we suspect that uncontrolled assembly of an unlinked additional subunit (in this case β_2) may be deleterious, but directed assembly may result in greater functional expression of the new nAChR subtype. Certainly, this study provides direct evidence that β_2 subunit incorporation into α_7*-nAChRs is compatible with agonist-induced function.

The pharmacological profiles of $\alpha_7\beta_2$-nAChRs were very similar to those of homopentameric α_7-nAChRs. Even agonists (sazetidine-A, CC4) and an antagonist (DHβE) previously shown to have significant β_2*-nAChR selectivity had indistinguishable pharmacology across homomeric α_7-nAChRs and the two different $\alpha_7\beta_2$-nAChR isoforms. Each of these findings matches those very recently published using *Xenopus* oocytes expressing α_7 and β_2 subunits at a 1:10 ratio (Zwart et al., 2014). The only statistically significant difference in this study was a diminution of nicotine's efficacy relative to that of ACh in the two $\alpha_7\beta_2$-nAChR isoforms (also seen by Zwart et al., 2014). This nicotine partial agonism further confirms that β_2 was incorporated into $\alpha_7\beta_2$-nAChR concatemers as planned and may represent a pharmacological marker for the presence of $\alpha_7\beta_2$-nAChRs. The same may be true of the slower desensitization kinetics measured for the $(\alpha_7)_3(\beta_2)_2$ (Fig. 3), although it is important to note the limitations of measuring receptor kinetics in a *Xenopus* oocyte system (Papke, 2010). We note that the similar α_7-nAChR versus $\alpha_7\beta_2$-nAChR potency of DHβE observed by us and by Zwart et al. (2014) does not match the observations made in two previous studies (Liu et al., 2009; Murray et al., 2012). The reason for this discrepancy between

TABLE 4

α_7 and $\alpha_7\beta_2$-nAChR agonist pharmacological parameters

Values are the mean ± S.E.M. of the number of indicated replicates (n=).

Subtype	ACh				Choline				Nicotine				Sazetidine-A				CC4			
	n=	$\log(EC_{50}/M)$	n_H	Efficacy	n=	$\log(EC_{50}/M)$	n_H	Efficacy	n=	$\log(EC_{50}/M)$	n_H	Efficacy	n=	$\log(EC_{50}/M)$	n_H	Efficacy	n=	$\log(EC_{50}/M)$	n_H	Efficacy
α_7 (unlinked)	6	−3.3 ± 0.2	1.3 ± 0.1	103 ± 3	3	−2.9 ± 0.04	1.9 ± 0.3	87 ± 4	3	−4.6 ± 0.14	2.7 ± 0.5	95 ± 2	3	ND	ND	3.0 ± 0.5	3	ND	ND	3.0 ± 1.0
α_7-α_7-α_7-α_7	6	−3.5 ± 0.3	1.3 ± 0.1	96 ± 2	3	−2.9 ± 0.17	1.6 ± 0.4	96 ± 8	3	−4.1 ± 0.15	1.7 ± 0.3	84 ± 4	3	ND	ND	7.0 ± 3.0	3	ND	ND	6.7 ± 1.6
α_7-α_7-β_2-α_7-α_7	6	−3.5 ± 0.03	1.3 ± 0.1	97 ± 2	3	−2.9 ± 0.03	1.8 ± 0.2	90 ± 3	3	−4.2 ± 0.15	1.9 ± 0.5	58 ± 3*	3	ND	ND	3.5 ± 0.5	3	ND	ND	3.2 ± 0.6
α_7-β_2-α_7-β_2-α_7	6	−3.3 ± 0.3	1.6 ± 0.3	99 ± 3	3	−2.9 ± 0.12	2.0 ± 0.2	95 ± 2	3	−4.2 ± 0.08	1.9 ± 0.6	55 ± 4*	3	ND	ND	3.4 ± 0.4	3	ND	ND	3.5 ± 1.0

Agonist $\log EC_{50}$, Hill slope (n_H), and efficacy values relative to a maximally effective (10 mM) concentration of ACh were derived by nonlinear least-squares curve fitting of the data shown in Fig. 4 to the Hill model. α_7-only nAChR expressed in *Xenopus* oocytes from unlinked subunits were used as a control group, to which the functional properties of α_7-nAChR concatemeric constructs were compared (N-to-C-terminal subunit orders are shown). Pharmacological parameters measured for each agonist were generally indistinguishable between all four groups of oocytes, with one exception: The relative efficacy of nicotine was lower for both $\alpha_7\beta_2$ subtypes tested compared with the α_7 unlinked control group (although the α_7-only concatemer group was not different to the control). One-way analysis of variance: $F_{[3,8]} = 34.2$, $P < 0.001$, followed by Dunnett's post hoc test (*$P < 0.05$). ND, not determinable (reliable curve fitting is not possible for very low-efficacy compounds).

the pairs of studies is not clear, but two possible explanations occur. First, the differences previously measured are relatively subtle, so they may be hard to reproduce. Related to this point, we note that the Hill slopes of the $\alpha_7\beta_2$-nAChR DHβE concentration response curves (Fig. 5A) are shallower than those measured for other competitive antagonists ($\leq$1, as opposed to significantly >1 for MLA and α-Cbtx). This would tend to obscure fine differences in IC_{50} values. Second, other α_7 and β_2 subunit associations are possible, in addition to those used in the $\alpha_7\beta_2$-nAChR concatemers deployed in this study. It is possible that an $\alpha_7\beta_2$*-nAChR population expressed from unlinked subunits may assemble differently, giving rise to the slightly different DHβE sensitivity previously measured. This would match the previous experience in which $\alpha_3\beta_4\alpha_5$-nAChR pharmacology perfectly matched between concatenated and unlinked-subunit nAChRs, but that of loose-subunit $\alpha_3\beta_4$-only nAChRs was close, but not identical, between loose-subunit and concatemeric constructs (George et al., 2012). Further work may be needed to understand the (admittedly subtle) pharmacological differences between alternative $\alpha_7\beta_2$-nAChR subunit stoichiometries and association orders.

Overall, however, the functional pharmacology of α_7-nAChR and $\alpha_7\beta_2$-nAChR subtypes is remarkably similar. This observation indirectly supports the concept that activation of $\alpha_7\beta_2$-nAChRs may be predominantly or exclusively mediated only through agonist binding sites at α_7/α_7 (not α_7/β_2) interfaces (Murray et al., 2012). If this is true, it seems unlikely that any competitive agonist could exhibit a significantly different potency between the α_7-nAChR and $\alpha_7\beta_2$-nAChR. However, antagonists capable of disrupting the allosteric transitions required for nAChR activation (Celie et al., 2005), and of selectively binding to α_7/β_2 interfaces, could be valuable in this regard as could other noncompetitive ligands. In the concatemeric $(\alpha_7)_4(\beta_2)_1$-nAChR construct (subunit order α_7-α_7-β_2-α_7-α_7), only three α_7/α_7 subunit interfaces will be retained (between the first two subunits, the last two subunits, and between the first and last subunits that will assemble together to complete the pentameric nAChR structure). In the $(\alpha_7)_3(\beta_2)_2$-nAChR construct, only the α_7/α_7 interface formed between the first and last subunits will be retained. At first glance, it may seem remarkable that an α_7*-nAChR containing such a diminished complement of putative agonist binding sites could be effectively activated. However, elegant recent work indicates that the nAChR, including α_7-nAChR, can be activated effectively by as few as one agonist binding site (Rayes et al., 2009; Williams et al., 2011; Andersen et al., 2013).

That $\alpha_7\beta_2$-nAChRs are relatively scarce in basal forebrain does not imply that their role is necessarily insignificant. For example, $\alpha_6\beta_2$*-nAChR expression on substantia nigra/ventral tegmental area dopamine projections comprises <10% of all β_2*-nAChRs in dopamine terminal regions (Whiteaker et al., 2000; Gotti et al., 2005), but this subtype is extremely important in controlling local neuronal behavior and signal processing (Exley and Cragg, 2008; Exley et al., 2008). Cholinergic neurons constitute only a fraction (10–15%) of basal forebrain neurons (Semba, 2000) and the proportion of a $\alpha_7\beta_2$-nAChRs in these neurons may therefore be relatively large. The basal forebrain cholinergic system provides primary cholinergic innervations to limbic and cortical brain structures, and expresses nAChRs that participate in the cholinergic transmission

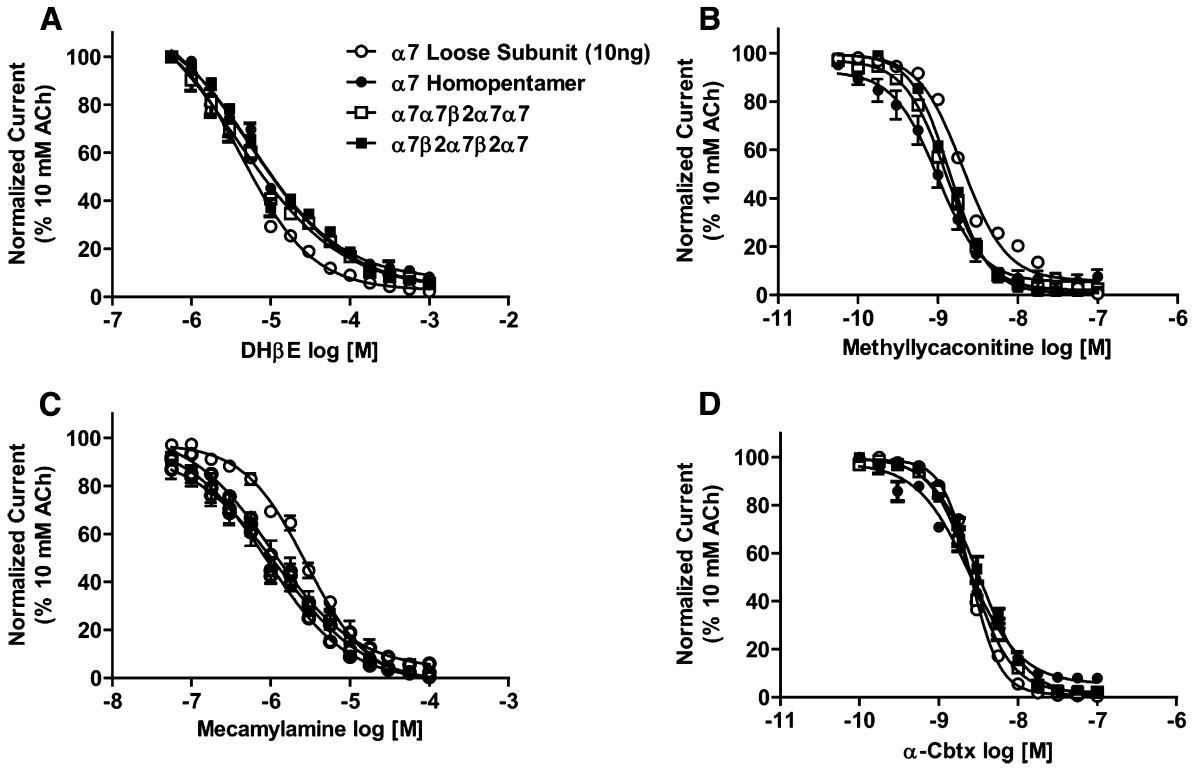

Fig. 5. Antagonist concentration response profiles for α_7- and $\alpha_7\beta_2$-nAChRs. Oocytes were injected with mRNA encoding unlinked α_7 subunits (○), concatenated α_7 homopentamers (●), or concatenated $\alpha_7\beta_2$ pentameric concatemers (□ indicates $\alpha_7\beta_2$ nAChR with the β_2 subunit in position 3; ■ indicates $\alpha_7\beta_2$ nAChR with the β_2 subunit in positions 2 and 4). Before antagonists were applied to each oocyte, a control 10 mM ACh-evoked response was measured. Oocytes were preperfused with the following nAChR antagonists: DHβE ($10^{-6.25}$ to 10^{-3}; $n = 3$) (A), methyllycaconitine ($10^{-10.5}$ to 10^{-7}; $n = 3$) (B), mecamylamine ($10^{-7.25}$ to 10^{-4}; $n = 3$) (C), or α-Cbtx (10^{-10} to 10^{-7}; $n = 3$) (D). The magnitudes of subsequent 10 mM ACh stimulations were compared with that of the initial control. Data points represent the mean ± S.E.M. Drug potency and efficacy parameters were calculated by nonlinear least-squares curve fitting to the Hill equation (see *Materials and Methods*). The resulting pharmacological parameters and statistical analyses are summarized in Table 5.

and cognitive processes associated with learning and memory (Voytko et al., 1994; Hernandez et al., 2010). One of the most marked pathologic changes in the brain in Alzheimer disease is the degeneration of this cholinergic projection and the consequent reduction in the number of nAChRs (Dumas and Newhouse, 2011; Pinto et al., 2011). A number of studies have found that the β-amyloid (Aβ) peptide (a hallmark of Alzheimer disease) plays a critical role in neuronal degeneration and subsequent memory deficits (Price et al., 1985; Holtzman et al., 1992; Wenk, 1993; Fraser et al., 1997; Capsoni et al., 2000; Dolga et al., 2009). Furthermore, a recent electrophysiological study has demonstrated that Aβ binds with higher affinity to $\alpha_7\beta_2$-nAChR than to α_7-nAChR, and that this can produce hippocampal neuronal hyperexcitation (through α_7-nAChR upregulation) and subsequent neurodegeneration (Liu et al., 2013).

Post mortem tissue is an underused substrate for genetic and/or preclinical studies, and provides a translational element that is difficult to recapitulate in animal models alone (McCullumsmith et al., 2014). This study's definitive evidence that $\alpha_7\beta_2$*-nAChRs are found in human as well as mouse basal forebrain provides valuable support for the concept that this subtype may be relevant to the study and etiology of Alzheimer disease. The similarities in human- and mouse-brain basal forebrain $\alpha_7\beta_2$*-nAChR expression are also supportive of the use of mouse models in this context.

TABLE 5

α_7 and $\alpha_7\beta_2$-nAChR antagonist pharmacological parameters

Values are the mean ± S.E.M. of the number of indicated replicates (n=).

Subtype	DHβE			MLA			Mecamylamine			α-Cbtx		
	n=	log(IC_{50}/M)	n_H	n=	log(IC_{50}/M)	n_H	n=	log(IC_{50} / M)	n_H	n=	log(IC_{50}/M)	n_H
α_7 (unlinked)	3	−5.2 ± 0.05	−1.0 ± 0.1	3	−8.7 ± 0.1	−1.6 ± 0.2	3	−5.6 ± 0.2		3	−8.6 ± 0.1	2.4 ± 0.5
α_7-α_7-α_7-α_7-α_7	3	−5.3 ± 0.07	−0.8 ± 0.1	3	−9.0 ± 0.1	−1.6 ± 0.2	3	−6.0 ± 0.2		3	−8.6 ± 0.1	1.3 ± 0.8
α_7-α_7-β_2-α_7-α_7	3	−5.4 ± 0.10	−0.6 ± 0.1	3	−8.9 ± 0.1	−1.7 ± 0.1	3	−6.0 ± 0.1		3	−8.6 ± 0.1	1.8 ± 0.5
α_7-β_2-α_7-β_2-α_7	3	−5.4 ± 0.10	−0.7 ± 0.1	3	−8.8 ± 0.1	−1.8 ± 0.1	3	−6.0 ± 0.2		3	−8.5 ± 0.2	1.5 ± 0.6

Antagonist log IC_{50} and Hill slope (n_H) values were derived by nonlinear least-squares curve fitting of the data shown in Fig. 5 to the Hill model. Pharmacological parameters obtained for each antagonist were statistically indistinguishable between all four groups of oocytes according to analysis with one-way analysis of variance.

Acknowledgments

The authors thank Dr. Emanuele Sher and Dr. Rudolf Zwart (Eli Lilly Company) for their continuous support and for supply of human basal forebrain samples. They also thank Dr. Jenny Court (Newcastle upon Tyne General Hospital) for supplying human cerebellum tissue. Cerebellum tissue for this study was provided by the Newcastle Brain Tissue Resource.

Authorship Contributions

Participated in research design: Zoli, George, Lukas, Whiteaker, Gotti.

Conducted experiments: Moretti, George, Pistillo.

Contributed new reagents or analytic tools: Pistillo, Maskos, Whiteaker.

Performed data analysis: Moretti, George, Pistillo, Whiteaker.

Wrote or contributed to the writing of the manuscript: Zoli, Lukas, Whiteaker, Gotti.

References

Albuquerque EX, Alkondon M, Pereira EFR, Castro NG, Schrattenholz A, Barbosa CTF, Bonfante-Cabarcas R, Aracava Y, Eisenberg HM, and Maelicke A (1997) Properties of neuronal nicotinic acetylcholine receptors: pharmacological characterization and modulation of synaptic function. *J Pharmacol Exp Ther* **280**: 1117–1136.

Albuquerque EX, Pereira EFR, Alkondon M, and Rogers SW (2009) Mammalian nicotinic acetylcholine receptors: from structure to function. *Physiol Rev* **89**:73–120.

Alkondon M, Pereira EFR, Cortes WS, Maelicke A, and Albuquerque EX (1997) Choline is a selective agonist of α7 nicotinic acetylcholine receptors in the rat brain neurons. *Eur J Neurosci* **9**:2734–2742.

Andersen N, Corradi J, Sine SM, and Bouzat C (2013) Stoichiometry for activation of neuronal α7 nicotinic receptors. *Proc Natl Acad Sci USA* **110**:20819–20824.

Azam L, Winzer-Serhan U, and Leslie FM (2003) Co-expression of α7 and β2 nicotinic acetylcholine receptor subunit mRNAs within rat brain cholinergic neurons. *Neuroscience* **119**:965–977.

Balestra B, Vailati S, Moretti M, Hanke W, Clementi F, and Gotti C (2000) Chick optic lobe contains a developmentally regulated alpha2alpha5beta2 nicotinic receptor subtype. *Mol Pharmacol* **58**:300–311.

Capsoni S, Ugolini G, Comparini A, Ruberti F, Berardi N, and Cattaneo A (2000) Alzheimer-like neurodegeneration in aged antinerve growth factor transgenic mice. *Proc Natl Acad Sci USA* **97**:6826–6831.

Carbone AL, Moroni M, Groot-Kormelink PJ, and Bermudez I (2009) Pentameric concatenated (alpha4)(2)(beta2)(3) and (alpha4)(3)(beta2)(2) nicotinic acetylcholine receptors: subunit arrangement determines functional expression. *Br J Pharmacol* **156**:970–981.

Celie PHN, Kasheverov IE, Mordvintsev DY, Hogg RC, van Nierop P, van Elk R, van Rossum-Fikkert SE, Zhmak MN, Bertrand D, and Tsetlin V et al. (2005) Crystal structure of nicotinic acetylcholine receptor homolog AChBP in complex with an alpha-conotoxin PnIA variant. *Nat Struct Mol Biol* **12**:582–588.

Conroy WG and Berg DK (1998) Nicotinic receptor subtypes in the developing chick brain: appearance of a species containing the alpha4, beta2, and alpha5 gene products. *Mol Pharmacol* **53**:392–401.

Court JA, Johnson M, Religa D, Keverne J, Kalaria R, Jaros E, McKeith IG, Perry R, Naslund J, and Perry EK (2005) Attenuation of Abeta deposition in the entorhinal cortex of normal elderly individuals associated with tabacco smoking. *neuropathol Appl Neurobiol* **31**:522–535.

Criado M, Valor LM, Mulet J, Gerber S, Sala S, and Sala F (2012) Expression and functional properties of α7 acetylcholine nicotinic receptors are modified in the presence of other receptor subunits. *J Neurochem* **123**:504–514.

Dajas-Bailador F and Wonnacott S (2004) Nicotinic acetylcholine receptors and the regulation of neuronal signalling. *Trends Pharmacol Sci* **25**:317–324.

Dolga AM, Granic I, Nijholt IM, Nyakas C, van der Zee EA, Luiten PG, and Eisel UL (2009) Pretreatment with lovastatin prevents N-methyl-D-aspartate-induced neurodegeneration in the magnocellular nucleus basalis and behavioral dysfunction. *J Alzheimers Dis* **17**:327–336.

Drisdel RC and Green WN (2000) Neuronal α-bungarotoxin receptors are α7 subunit homomers. *J Neurosci* **20**:133–139.

Dumas JA and Newhouse PA (2011) The cholinergic hypothesis of cognitive aging revisited again: cholinergic functional compensation. *Pharmacol Biochem Behav* **99**:254–261.

Eaton JB, Lucero LM, Stratton H, Chang Y, Cooper JF, Lindstrom JM, Lukas RJ, and Whiteaker P (2014) The unique α4+/-α4 agonist binding site in (α4)3(β2)2 subtype nicotinic acetylcholine receptors permits differential agonist desensitization pharmacology versus the (α4)2(β2)3 subtype. *J Pharmacol Exp Ther* **348**:46–58.

Exley R, Clements MA, Hartung H, McIntosh JM, and Cragg SJ (2008) Alpha6-containing nicotinic acetylcholine receptors dominate the nicotine control of dopamine neurotransmission in nucleus accumbens. *Neuropsychopharmacology* **33**: 2158–2166.

Exley R and Cragg SJ (2008) Presynaptic nicotinic receptors: a dynamic and diverse cholinergic filter of striatal dopamine neurotransmission. *Br J Pharmacol* **153** (Suppl 1):S283–S297.

Flora A, Schulz R, Benfante R, Battaglioli E, Terzano S, Clementi F, and Fornasari D (2000) Neuronal and extraneuronal expression and regulation of the human alpha5 nicotinic receptor subunit gene. *J Neurochem* **75**:18–27.

Fraser SP, Suh YH, and Djamgoz MB (1997) Ionic effects of the Alzheimer's disease beta-amyloid precursor protein and its metabolic fragments. *Trends Neurosci* **20**: 67–72.

George AA, Lucero LM, Damaj MI, Lukas RJ, Chen X, and Whiteaker P (2012) Function of human α3β4α5 nicotinic acetylcholine receptors is reduced by the α5 (D398N) variant. *J Biol Chem* **287**:25151–25162.

Girod R, Crabtree G, Ernstrom G, Ramirez-Latorre J, McGehee D, Turner J, and Role L (1999) Heteromeric complexes of alpha 5 and/or alpha 7 subunits. Effects of calcium and potential role in nicotine-induced presynaptic facilitation. *Ann N Y Acad Sci* **868**:578–590.

Gotti C and Clementi F (2004) Neuronal nicotinic receptors: from structure to pathology. *Prog Neurobiol* **74**:363–396.

Gotti C, Hanke W, Maury K, Moretti M, Ballivet M, Clementi F, and Bertrand D (1994) Pharmacology and biophysical properties of α 7 and α 7-α 8 α-bungarotoxin receptor subtypes immunopurified from the chick optic lobe. *Eur J Neurosci* **6**: 1281–1291.

Gotti C, Moretti M, Bohr I, Ziabreva I, Vailati S, Longhi R, Riganti L, Gaimarri A, McKeith IG, and Perry RH et al. (2006) Selective nicotinic acetylcholine receptor subunit deficits identified in Alzheimer's disease, Parkinson's disease and dementia with Lewy bodies by immunoprecipitation. *Neurobiol Dis* **23**:481–489.

Gotti C, Moretti M, Clementi F, Riganti L, McIntosh JM, Collins AC, Marks MJ, and Whiteaker P (2005) Expression of nigrostriatal alpha 6-containing nicotinic acetylcholine receptors is selectively reduced, but not eliminated, by beta 3 subunit gene deletion. *Mol Pharmacol* **67**:2007–2015.

Grady SR, Moretti M, Zoli M, Marks MJ, Zanardi A, Pucci L, Clementi F, and Gotti C (2009) Rodent habenulo-interpeduncular pathway expresses a large variety of uncommon nAChR subtypes, but only the alpha3beta4* and alpha3beta3beta4* subtypes mediate acetylcholine release. *J Neurosci* **29**:2272–2282.

Griguoli M and Cherubini E (2012) Regulation of hippocampal inhibitory circuits by nicotinic acetylcholine receptors. *J Physiol* **590**:655–666.

Halevi S, McKay J, Palfreyman M, Yassin L, Eshel M, Jorgensen E, and Treinin M (2002) The C. elegans ric-3 gene is required for maturation of nicotinic acetylcholine receptors. *EMBO J* **21**:1012–1020.

Hernandez CM, Kayed R, Zheng H, Sweatt JD, and Dineley KT (2010) Loss of alpha7 nicotinic receptors enhances beta-amyloid oligomer accumulation, exacerbating early-stage cognitive decline and septohippocampal pathology in a mouse model of Alzheimer's disease. *J Neurosci* **30**:2442–2453.

Holtzman DM, Li YW, DeArmond SJ, McKinley MP, Gage FH, Epstein CJ, and Mobley WC (1992) Mouse model of neurodegeneration: atrophy of basal forebrain cholinergic neurons in trisomy 16 transplants. *Proc Natl Acad Sci USA* **89**: 1383–1387.

Hurst R, Rollema H, and Bertrand D (2013) Nicotinic acetylcholine receptors: from basic science to therapeutics. *Pharmacol Ther* **137**:22–54.

Keyser KT, Britto LRG, Schoepfer R, Whiting P, Cooper J, Conroy W, Brozozowska-Prechtl A, Karten HJ, and Lindstrom J (1993) Three subtypes of alpha-bungarotoxin-sensitive nicotinic acetylcholine receptors are expressed in chick retina. *J Neurosci* **13**:442–454.

Khiroug SS, Harkness PC, Lamb PW, Sudweeks SN, Khiroug L, Millar NS, and Yakel JL (2002) Rat nicotinic ACh receptor α7 and β2 subunits co-assemble to form functional heteromeric nicotinic receptor channels. *J Physiol* **540**:425–434.

Kozikowski AP, Eaton JB, Bajjuri KM, Chellappan SK, Chen Y, Karadi S, He R, Caldarone B, Manzano M, and Yuen PW et al. (2009) Chemistry and pharmacology of nicotinic ligands based on 6-[5-(azetidin-2-ylmethoxy)pyridin-3-yl]hex-5-yn-1-ol (AMOP-H-OH) for possible use in depression. *ChemMedChem* **4**:1279–1291.

Kuryatov A and Lindstrom J (2011) Expression of functional human α6β2β3* acetylcholine receptors in Xenopus laevis oocytes achieved through subunit chimeras and concatamers. *Mol Pharmacol* **79**:126–140.

Lendvai B and Vizi ES (2008) Nonsynaptic chemical transmission through nicotinic acetylcholine receptors. *Physiol Rev* **88**:333–349.

Lewis AS and Picciotto MR (2013) High-affinity nicotinic acetylcholine receptor expression and trafficking abnormalities in psychiatric illness. *Psychopharmacology (Berl)* **229**:477–485.

Liu Q, Huang Y, Shen JX, Steffensen S, and Wu J (2012) Functional α7β2 nicotinic acetylcholine receptors expressed in hippocampal interneurons exhibit high sensitivity to pathological level of amyloid β peptides. *BMC Neurosci* **13**:155.

Liu Q, Huang Y, Xue F, Simard A, DeChon J, Li G, Zhang J, Lucero L, Wang M, and Sierks M et al. (2009) A novel nicotinic acetylcholine receptor subtype in basal forebrain cholinergic neurons with high sensitivity to amyloid peptides. *J Neurosci* **29**:918–929.

Liu Q, Xie X, Lukas RJ, St John PA, and Wu J (2013) A novel nicotinic mechanism underlies β-amyloid-induced neuronal hyperexcitation. *J Neurosci* **33**:7253–7263.

Lukas RJ, Changeux JP, Le Novère N, Albuquerque EX, Balfour DJK, Berg DK, Bertrand D, Chiappinelli VA, Clarke PBS, and Collins AC et al. (1999) International Union of Pharmacology. XX. Current status of the nomenclature for nicotinic acetylcholine receptors and their subunits. *Pharmacol Rev* **51**:397–401.

Mazzaferro S, Benallegue N, Carbone A, Gasparri F, Vijayan R, Biggin PC, Moroni M, and Bermudez I (2011) Additional acetylcholine (ACh) binding site at α4/α4 interface of (α4β2)2α4 nicotinic receptor influences agonist sensitivity. *J Biol Chem* **286**:31043–31054.

McCullumsmith RE, Hammond JH, Shan D, and Meador-Woodruff JH (2014) Postmortem brain: an underutilized substrate for studying severe mental illness. *Neuropsychopharmacology* **39**:65–87.

Murray TA, Bertrand D, Papke RL, George AA, Pantoja R, Srinivasan R, Liu Q, Wu J, Whiteaker P, and Lester HA et al. (2012) α7β2 nicotinic acetylcholine receptors assemble, function, and are activated primarily via their α7-α7 interfaces. *Mol Pharmacol* **81**:175–188.

Orr-Urtreger A, Göldner FM, Saeki M, Lorenzo I, Goldberg L, De Biasi M, Dani JA, Patrick JW, and Beaudet AL (1997) Mice deficient in the α7 neuronal nicotinic acetylcholine receptor lack α-bungarotoxin binding sites and hippocampal fast nicotinic currents. *J Neurosci* **17**:9165–9171.

Palma E, Maggi L, Barabino B, Eusebi F, and Ballivet M (1999) Nicotinic acetylcholine receptors assembled from the α7 and β3 subunits. *J Biol Chem* **274**:18335–18340.
Papke RL (2010) Tricks of perspective: insights and limitations to the study of macroscopic currents for the analysis of nAChR activation and desensitization. *Mol Neurosci J* **401**:77–86.
Picciotto MR, Higley MJ, and Mineur YS (2012) Acetylcholine as a neuromodulator: cholinergic signaling shapes nervous system function and behavior. *Neuron* **76**:116–129.
Picciotto MR, Zoli M, Léna C, Bessis A, Lallemand Y, Le Novère N, Vincent P, Pich EM, Brûlet P, and Changeux JP (1995) Abnormal avoidance learning in mice lacking functional high-affinity nicotine receptor in the brain. *Nature* **374**:65–67.
Pinto T, Lanctôt KL, and Herrmann N (2011) Revisiting the cholinergic hypothesis of behavioral and psychological symptoms in dementia of the Alzheimer's type. *Ageing Res Rev* **10**:404–412.
Price DL, Cork LC, Struble RG, Whitehouse PJ, Kitt CA, and Walker LC (1985) The functional organization of the basal forebrain cholinergic system in primates and the role of this system in Alzheimer's disease. *Ann N Y Acad Sci* **444**:287–295.
Rayes D, De Rosa MJ, Sine SM, and Bouzat C (2009) Number and locations of agonist binding sites required to activate homomeric Cys-loop receptors. *J Neurosci* **29**: 6022–6032.
Riganti L, Matteoni C, Di Angelantonio S, Nistri A, Gaimarri A, Sparatore F, Canu-Boido C, Clementi F, and Gotti C (2005) Long-term exposure to the new nicotinic antagonist 1,2-bisN-cytisinylethane upregulates nicotinic receptor subtypes of SH-SY5Y human neuroblastoma cells. *Br J Pharmacol* **146**:1096–1109.
Sala M, Braida D, Pucci L, Manfredi I, Marks MJ, Wageman CR, Grady SR, Loi B, Fucile S, and Fasoli F et al. (2013) CC4, a dimer of cytisine, is a selective partial agonist at α4β2/α6β2 nAChR with improved selectivity for tobacco smoking cessation. *Br J Pharmacol* **168**:835–849.
Schneider CA, Rasband WS, and Eliceiri KW (2012) NIH Image to ImageJ: 25 years of image analysis. *Nat Methods* **9**:671–675.
Semba K (2000) Multiple output pathways of the basal forebrain: organization, chemical heterogeneity, and roles in vigilance. *Behav Brain Res* **115**:117–141.
Stokes C and Papke RL (2012) Use of an α3β4 nicotinic acetylcholine receptor subunit concatamer to characterize ganglionic receptor subtypes with specific subunit composition reveals species-specific pharmacologic properties. *Neuropharmacology* **63**:538–546.
Voytko ML, Olton DS, Richardson RT, Gorman LK, Tobin JR, and Price DL (1994) Basal forebrain lesions in monkeys disrupt attention but not learning and memory. *J Neurosci* **14**:167–186.
Wenk GL (1993) A primate model of Alzheimer's disease. *Behav Brain Res* **57**: 117–122.
Whiteaker P, Christensen S, Yoshikami D, Dowell C, Watkins M, Gulyas J, Rivier J, Olivera BM, and McIntosh JM (2007) Discovery, synthesis, and structure activity of a highly selective alpha7 nicotinic acetylcholine receptor antagonist. *Biochemistry* **46**:6628–6638.
Whiteaker P, McIntosh JM, Luo S, Collins AC, and Marks MJ (2000) 125I-alpha-conotoxin MII identifies a novel nicotinic acetylcholine receptor population in mouse brain. *Mol Pharmacol* **57**:913–925.
Williams DK, Stokes C, Horenstein NA, and Papke RL (2011) The effective opening of nicotinic acetylcholine receptors with single agonist binding sites. *J Gen Physiol* **137**:369–384.
Xiao Y, Fan H, Musachio JL, Wei ZL, Chellappan SK, Kozikowski AP, and Kellar KJ (2006) Sazetidine-A, a novel ligand that desensitizes alpha4beta2 nicotinic acetylcholine receptors without activating them. *Mol Pharmacol* **70**:1454–1460.
Yakel J (2013) Cholinergic receptors: functional role of nicotinic ACh receptors in brain circuits and disease. *Pflugers Arch* **465**:441–450.
Zhang X, Liu C, Miao H, Gong ZH, and Nordberg A (1998) Postnatal changes of nicotinic acetylcholine receptor alpha 2, alpha 3, alpha 4, alpha 7 and beta 2 subunits genes expression in rat brain. *Int J Dev Neurosci* **16**:507–518.
Zhou Y, Nelson ME, Kuryatov A, Choi C, Cooper J, and Lindstrom J (2003) Human alpha4beta2 acetylcholine receptors formed from linked subunits. *J Neurosci* **23**: 9004–9015.
Zoli M, Le Novère N, Hill JA, Jr, and Changeux JP (1995) Developmental regulation of nicotinic ACh receptor subunit mRNAs in the rat central and peripheral nervous systems. *J Neurosci* **15**:1912–1939.
Zwart R, Strotton M, Ching J, Astles PC, and Sher E (2014) Unique pharmacology of heteromeric α7β2 nicotinic acetylcholine receptors expressed in Xenopus laevis oocytes. *Eur J Pharmacol* **726**:77–86.

Address correspondence to: Dr. Cecilia Gotti, CNR Institute of Neurosience, Via Vanvitelli 32, 20129 Milan, Italy; or Dr. Paul Whiteaker, Division of Neurobiology, Barrow Neurologic Institute, St. Joseph's Hospital and Medical Center, 350 W. Thomas Rd., Phoenix, AZ 85013. E-mail: c.gotti@in.cnr or paul.whiteaker@dignityhealth.org